The latest SORCE Solar Spectral Irradiance Data Release: Inter-comparison of measurements

Laura Sandoval, Stéphane Béland, Jerald Harder, Erik Richard, and Thomas Woods

University of Colorado Boulder – Laboratory for Atmospheric and Space Physics (LASP)

I. Introduction

The Spectral Irradiance Monitor (SIM), the SOlar Stellar Irradiance Comparison Experiment (SOLSTICE), the XUV Photometer System (XPS), and the Total Irradiance Monitor (TIM) instruments on board the Solar Radiation and Climate Experiment (SORCE) satellite have been taking daily solar spectral irradiance (SSI) measurements since April 2003.

The SORCE satellite has been operating in Day Only Operations (DO-Op) mode since 2014 due to aging batteries. In addition to recalibrating the most recent data to account for instrument degradation, we addressed anomalies detected in the irradiance measurements taken by the SIM instrument, particularly those most apparent in the post DO-Op timeframe. We describe improvements in the new datasets and provide an inter-comparison of the SIM and TIM instruments and the NRLSSI2 model.

II. Methods and Results

A. Degradation Methods

The SIM instrument consists of two identical channels, each with UV, VIS, and IR photodiodes and ESR detectors. A back-aluminized prism disperses light on the focal plane where the co-aligned detectors are mounted. The ESR is robust and stable, but requires long integrations at each wavelength step to achieve an adequate signal to noise ratio. Conversely, the photodiodes have a fast response time, but are sensitive to temperature fluctuations and degradation in the space environment. The calibrated data from the ESR is used to determine the detector degradation as a function of time and wavelength.

$$correctedIrrad(\lambda,t) = \frac{uncorrectedIrrad}{pd * detectorDegradation}$$

During measurements the prism is exposed to unfiltered energetic solar radiation, inducing polymerization of the contaminants on its surface, resulting in a wavelength dependent reduction of optical transmission. By using two channels with different exposure rates we track the prim degradation as a function of solar exposure. The prism degradation (pd) for each channel is obtained using the following equation, where t_{expos} is the cumulative solar exposure for the channel under consideration, κ is the wavelength dependent absorption factor of the material on the prism, and f' is the time variability of the degradation. The $a_{detector}$ factor takes into account the geometry of the optical path in and out of the prism, as shown in Figure 1. The values for κ are calculated by minimizing the differences in the corrected irradiance between the two channels, at each wavelength using their respective known cumulative solar exposure and $a_{detector}$.

$$pd(\lambda,t) = (1-a_{detector}) \bullet exp(-\kappa\, t_{expos} \bullet f') + a_{detector} \bullet exp\left(\frac{-\kappa\, t_{expos} \bullet f'}{2}\right)$$

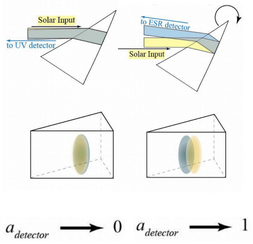

Figure 1. The raypath ($a_{detector}$) defines the fraction of the beam hitting the degradation spot on the way in and out of the prism.

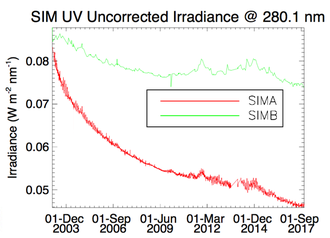

Figure 2. The uncorrected irradiance from Channel A and Channel B at 280.1 nm. Channel B has seen about 25% of the amount of solar exposure Channel A received.

The value of κ was evaluated over a time period where the instrument and the operations were very stable. This generates an average but fix value of $\kappa(\lambda)$ for the whole mission. The amount of outgassing material inside the instrument cavity is time-dependent such that one hour of solar exposure early in the mission produces higher degradation than one hour of exposure later in the mission. We compared the slopes of the corrected irradiance from both channels between coincident measurements. Changes in the ratios of the slopes provide a measurement of the time variability. This is performed one wavelength at a time for the whole mission, so that the f' is a function of both λ and t.

$$\frac{correctedIrrad_{A0}}{correctedIrrad_{A1}} = \frac{correctedIrrad_{B0}}{correctedIrrad_{B1}}$$

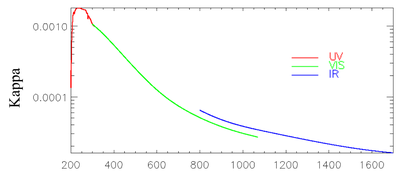

Figure 3. Average kappas as a function of wavelength.

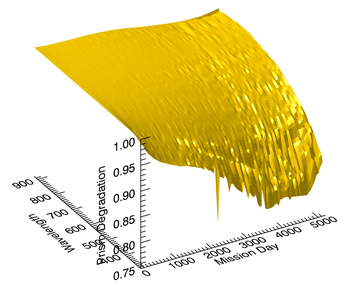

Figure 4. 3D plot of prism degradation in the VIS wavelength band.

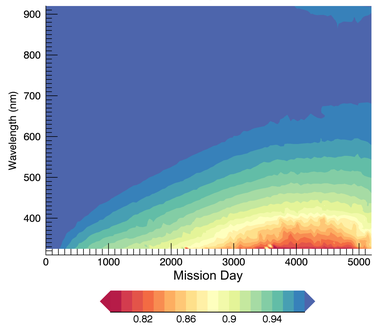

Figure 5. Contour plot of prism degradation in the VIS wavelength band.

B. Improvements in DO-Op

Since DO-Op mode SORCE makes solar observations during the daylight part of the orbit and goes into safe-hold every eclipse. This limitation requires multiple consecutive SIM measurements to be pieced together to generate a full spectrum. We noticed fluctuations in the irradiance during DO-Op mode and discovered outliers present in the data numbers. These outliers were the result of the mean being taken of an oversized dataset.

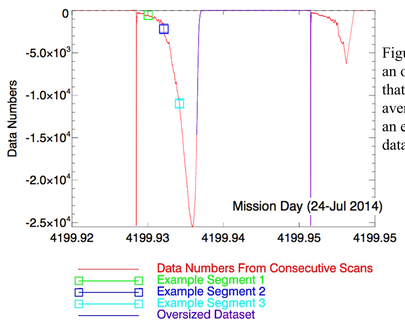

Figure 6. Example of an oversized dataset that was being averaged resulting in an erroneous mean data number.

The data was improved by removing the data number outliers, as shown in Figure 7.

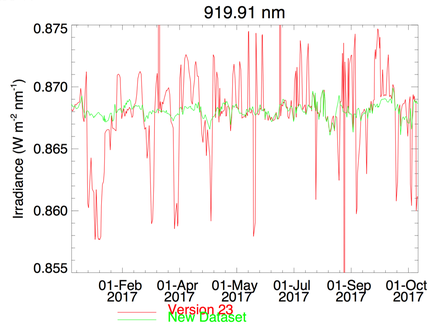

Figure 7. New dataset after the outliers in data numbers were identified and corrected compared with the previous version.

Temperature fluctuations were more prevalent in the DO-Op mode compared with earlier in the mission. The changes in temperature had the largest impact on the IR diode, especially at longer wavelengths, as shown in Figure 8. As a result of this finding we improved the temperature correction for the IR diode.

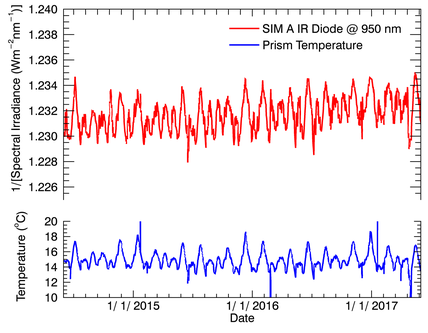

Figure 8. Demonstration of effect of temperature fluctuations on the IR diode in DO-Op mode.

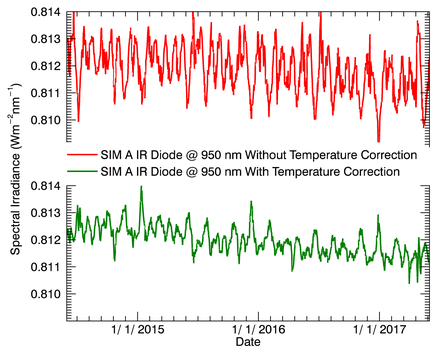

Figure 9. Before (top) and after (bottom) the temperature correction was made.

C. Results

The result of the corrections is apparent at individual wavelengths and in the TSI.

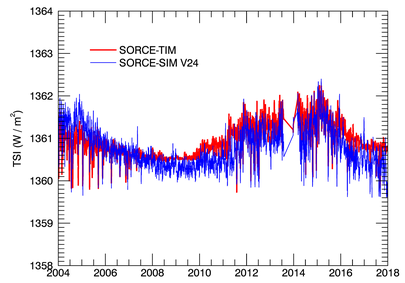

Figure 10. TSI comparison of SORCE-SIM V24 with SORCE-TIM

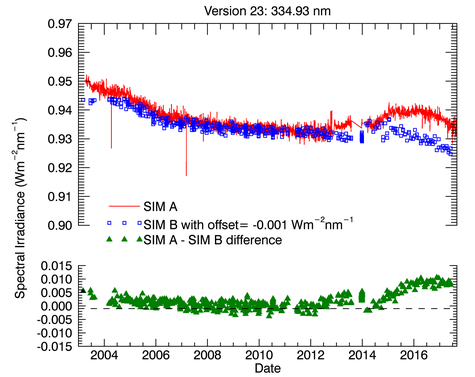

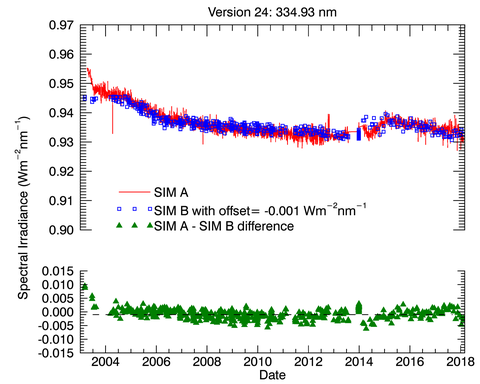

Figure 11. V23 VIS diode at 334 nm SIMA and SIM B agreement (top) compared with the agreement between SIMA and SIMB for V24 (bottom)

The integrated irradiance over specific wavelength regions are plotted in Figure 12 and compared with the proxy-based NRLSSI2 data. There is improved agreement between the NRLSSI2 model and Version 24 compared with Version 23.

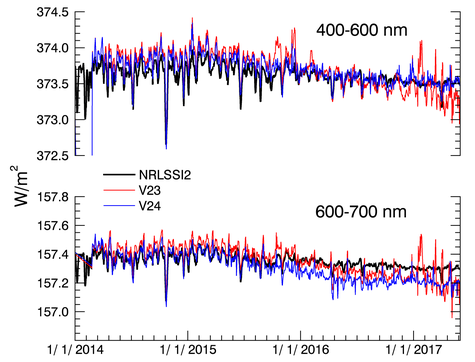

Figure 12. The integrated SSI over two wavelength regions. These results are compared with the NRLSSI2 model which uses a set of proxies to determine the SSI variability for the same wavelength ranges.

III. Conclusion

The improvements made for the SORCE-SIM dataset include the removal of data number outliers that were causing data irregularities, an improved temperature correction, and the extension of the degradation model to the most recent data in the DO-Op mode. These changes improved agreement with the NRLSSI2 model. The TSIS-1 satellite provides a continuation of the TIM and SIM measurements and has been taking its first light measurements since March 2018. The anticipated data from TSIS-SIM will provide a way to validate the SORCE-SIM data.